CHAPTER IV

A SIMPLE ROUTE TO BISMUTH TITANATE FROM BISMUTH GLYCOLATE PRECURSOR VIA SOL-GEL PROCESS

4.1 Abstract

Bismuth titanate ($Bi_4Ti_3O_{12}$) is successfully synthesized using bismuth glycolate as a bismuth source and acetic acid and ethanol as solvents via sol–gel process without adding a complexing agent. The synthesis parameters investigated are acetic acid to ethanol ratio, mechanical stirring time, calcination time and temperature. It is found that an increase in the acetic acid to ethanol ratio causes an increase in the gelation time, and the calcination temperature is the key factor in transformation to a crystalline $Bi_4Ti_3O_{12}$ perovskite phase. The perovskite phase of $Bi_4Ti_3O_{12}$ in a nanoplate shape is obtained after stirring the precursor mixture solution containing 0.1 acetic acid to ethanol ratio for 1 h at room temperature, followed by calcination of the dried gel at 600 °C for 1 h.

4.2 Introduction

Bismuth titanate ($Bi_4Ti_3O_{12}$) belongs to the Aurivillius family, which is composed of three perovskite-like $(Bi_2Ti_3O_{10})^{2-}$ layers sandwiched between $(Bi_2O_2)^{2+}$ layers.[1] Owing to its high Curie temperature, high breakdown strength and low dielectric dissipation factor, this material has attracted great attention as a potential candidate for electronic applications, such as non-volatile flash random memory devices or optical displays.[2–4] It can be synthesised by various methods, such as solid state,[5] hydrothermal,[6] metalorganic decomposition,[7] coprecipitation[8] and sol–gel process[9,10] techniques. Compared with the conventional solid state reaction, the sol–gel process has superior properties, namely better homogeneity, ease for controlling the composition and low formation temperature.[11,12] Bismuth alkoxide, first recognised within the last two decades, has become an important precursor.

It can be synthesised by several methods, such as metathesis reaction,[13] alcohol–alcohol exchange[14] and alcohol–amine exchange.[15]

Goia et al. reported that heating bismuth salts in polyol, such as ethylene glycol (EG) or propylene glycol, at 140–150°C yielded bismuth glycolate as an intermediate.[16] In agreement with Li et al., they also obtained bismuth glycolate during the synthesis of bismuth nanosphere by heating bismuth nitrate in EG at 185 °C without polyvinyl pyrolidone.[17]

In this work, a simple route to $Bi_4Ti_3O_{12}$ was examined with no complexing agent, using bismuth glycolate precursor directly synthesised by heating bismuth nitrate salt in EG in the presence of triethanolamine (TEA) as a catalyst. The synthesis parameters, namely acetic acid to ethanol ratio, mechanical stirring time, calcination time and temperature were also investigated.

4.3 Experimental

4.3.1 Materials

Bismuth nitrate pentahydrate ($Bi(NO_3)_3.5H_2O$) was purchased from UNIVAR Co. Triethanolamine ($N(CH_2CH_2OH)_3$) was supplied by QRëC Co. Ethylene glycol ($HOCH_2CH_2OH$) and ethanol (CH_3CH_2OH) were purchased from J.T. Baker Inc. Glacial acetic acid (CH_3COOH) and acetonitrile (CH_3CN) were purchased from RCI Labscan Co.Ltd. Titanium butoxide ($Ti(OCH_2CH_2CH_2CH_3)_4$) was obtained from Sigma-Aldrich Co. All chemicals were used as received.

4.3.2 Bismuth Glycolate Synthesis

Bismuth nitrate pentahydrate was dissolved in EG in a 250 mL round bottom flask and magnetically stirred until a clear solution was obtained. Triethanolamine was then added. The mixture was heated at 100 °C under nitrogen atmosphere for 2 h to obtain white precipitate. The precipitate was washed three times with acetronitrile, dried overnight in vacuum desiccators at room temperature and kept in vacuum desiccators for further characterisation.

4.3.3 Bismuth Titanate Preparation

The Bismuth glycolate (0.45 g) and titanium butoxide (0.35 g), used as bismuth and titanium sources respectively, were mixed in acetic acid and ethanol mixture (2.5 mL). The mixture was stirred at room temperature for 1, 3 or 6 h to obtain gel. The gel was then dried at 80°C for 6 h to obtain white powder, followed by calcination at temperatures in a range of 300–700°C. The optimal calcination temperature obtained was used to study an optimal calcination time.

4.3.4 Characterization

A Fourier transform infrared spectrometer (FT-IR;Nicolet iS10) was used to investigate the chemical structure of organic functionality using a resolution of 4 cm^{-1}. Thermogravimetric–derivative thermal analyzer (Perkin Elmer-Pyris Diamond) was employed to study the thermal property of the samples, using a heating rate of 10°C min^{-1} over a temperature range of 30–750°C in flowing inert N_2 atmosphere and a platinum pan. Solid state carbon-13 nuclear magnetic resonance spectrum was done on Varian-INOVA 13C-NMR-500 MHz. Mass spectrum was recorded on a gas chromatography–mass spectrometer (micrOTOF-Bruker Daltonics) equipped with Positive-ESI source and run in a range of 50–3000 m/z. A field emission scanning electron microscope (Hitachi/S-4800) was used to observe the morphology appearance of the samples by coating with a thin layer of platinum. The crystalline structure of the samples was analyzed on an X-ray diffractometer (XRD, Rigaku-RINT-2200) using CuKα source (1.5406 Å) with a scan speed of 5° (2θ)/min and a scan step of 0.02 (2θ) in a 5° to 60° (2θ) range.

4.4 Results and Discussion

4.4.1 Bismuth glycolate synthesis

Bismuth glycolate was synthesised by heating bismuth nitrate pentahydrate in EG under nitrogen atmosphere using TEA as a catalyst. Figure 4.1 shows the FT-IR spectra of EG and bismuth glycolate. Peaks at 3200–3500 (OH stretching), 1460–1380 (C–H stretching), 1089–1038 (C–O symmetric

stretching), 866 (C–H stretching) and 639 cm^{-1} (C–O–H bending) were observed. The as synthesised bismuth glycolate also gave peaks at 1384 cm^{-1}, belonging to adsorbed free NO_3^- ion on the surface,[18] and 580 cm^{-1}, corresponding to Bi-OR stretching of bismuth ethylene glycolate.[19]

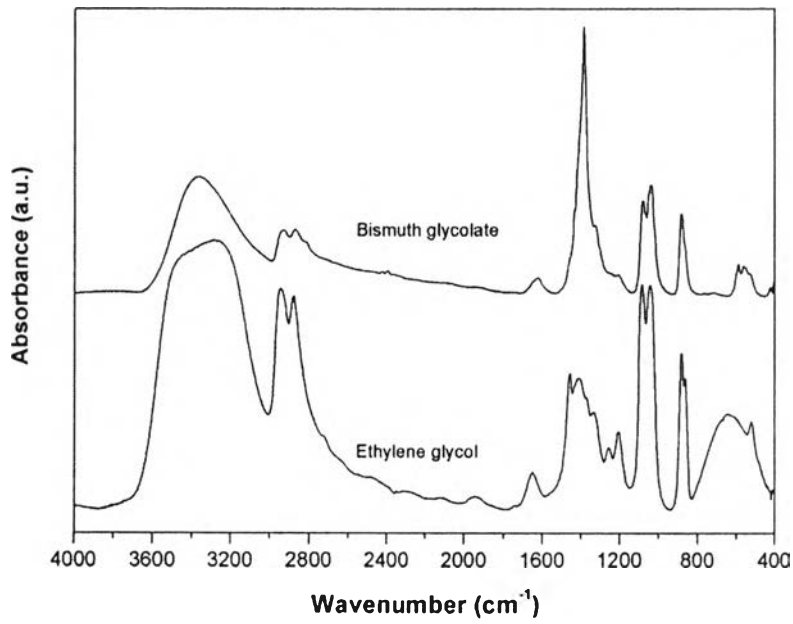

Figure 4.1 FT-IR spectra of ethylene glycol and bismuth glycolate.

Thermogravimetric–derivative thermal analysis shown in Figure 4.2a indicated two regions of weight loss, at 100–250 and 278 °C. The first weight loss was attributed to the trace amount of water and unreacted EG, while the second one at 278 °C corresponded to the decomposition of EG–ligands in bismuth glycolate structure. The final ceramic yield obtained was 64.9% with 35.1% weight loss. The ceramic yield could be inferred from the structure of $Bi_2(OCH_2CH_2O)(OCH_2CH_2OH)_4$, which gives a percent weight loss of 35.5 with 64.5% ceramic yield.

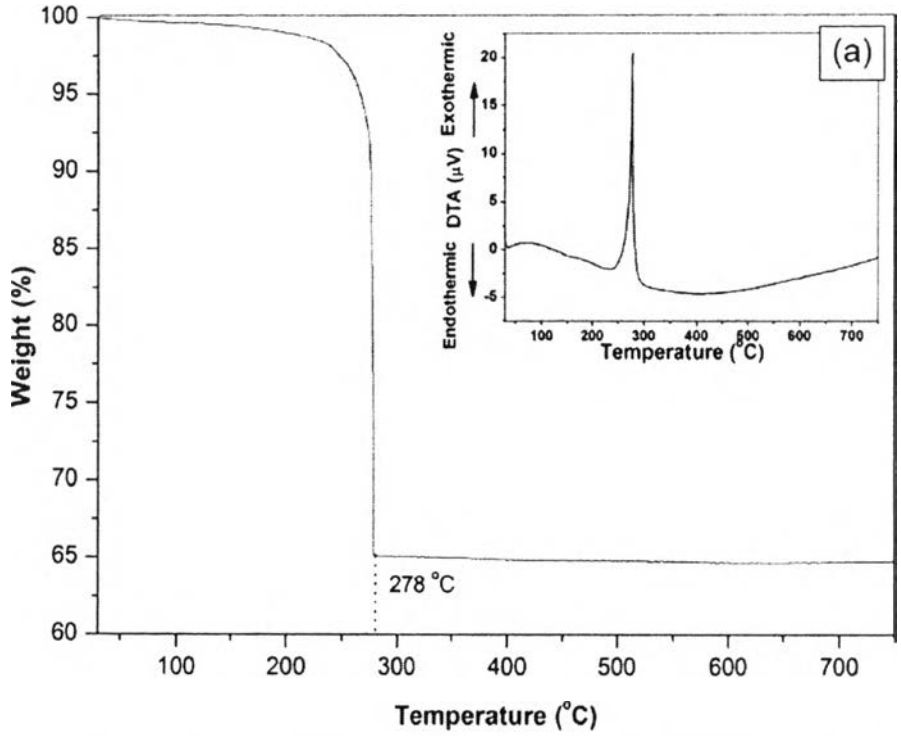
(a)
Weight (%)
Temperature (°C)
278 °C
Endothermic DTA (μV) Exothermic
Temperature (°C)

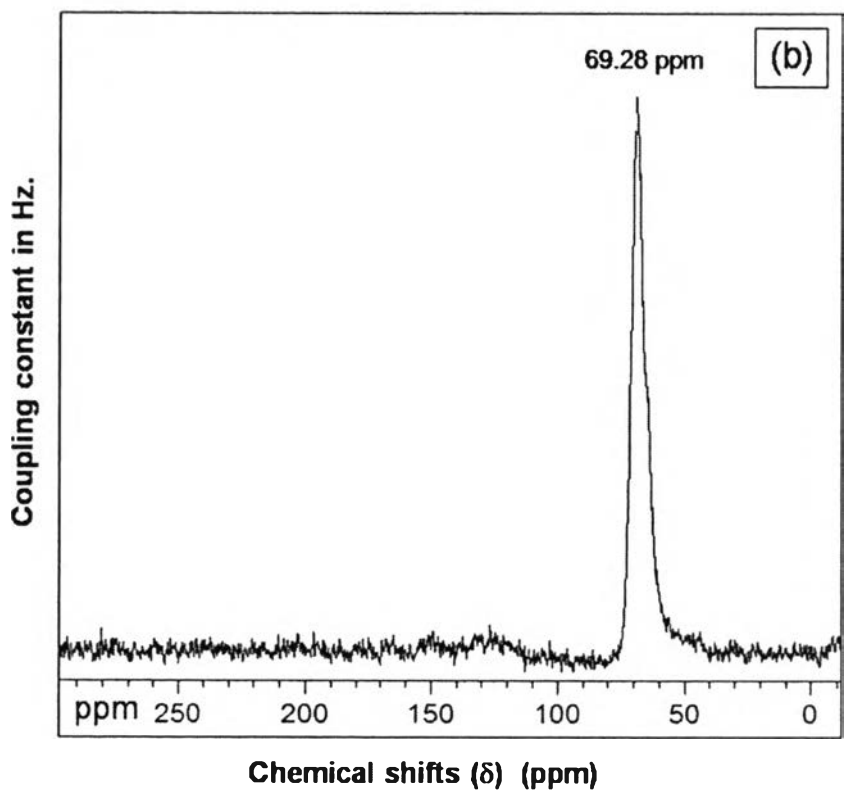
(b)
69.28 ppm
Coupling constant in Hz.
ppm
Chemical shifts (δ) (ppm)

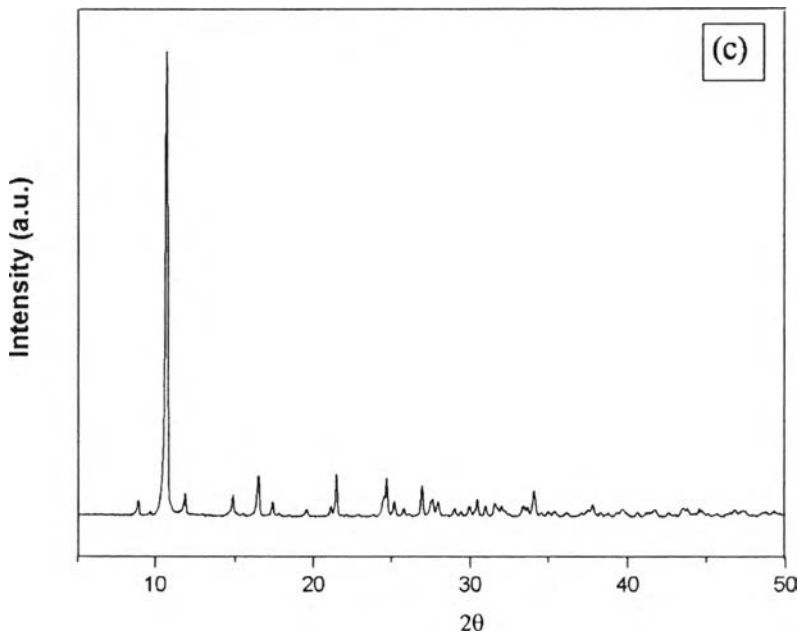

Figure 4.2 TG-DTA, Solid state ^{13}C-NMR, and XRD results of bismuth glycolate.

To confirm the bismuth glycolate structure, solid state ^{13}C-NMR was carried out, as can be seen in Figure 4.2b, which shows only one sharp peak centred at ~ 69.28 ppm. The peak is the characteristic peak of glycolate ligand, which is shifted from the standard peak of EG appearing at 63.4 ppm due to the influence of the Bi atom. There is no evidence of TEA participating in the bismuth glycolate structure, implying that it acted only as a catalyst in the process. Moreover, gas chromatography–mass spectrometry results, as summarized in Table 1, also indicated the fragmented structures containing EG–ligands bonding to the Bi atom. The crystallinity of bismuth glycolate was also observed in the XRD spectrum shown in Figure 4.2c. Bismuth glycolate powder mainly exhibited a strong low angle peak around 10–11° (2h). This is a specific feature of metal glycolate, such as cobalt glycolate,[20] manganese or lithium glycolate.[21]

Table 4.1 Proposed structure of fragmented bismuth glycolate

m/z	Intensity (%)	Proposed structure
583	32.7	-[CH_2CH_2OBi-OCH_2CH_2O-$BiOCH_2CH_2OH$]-
538	3.2	-[$Bi(OCH_2CH_2O)]_2^+$
376	37.5	-[H_3CH_2CO-Bi-$(OCH_2CH_2OH]_2^+$
347	100.0	-[OBi-$(OCH_2CH_2OH)_2$]

4.4.2 Bismuth Titanate Synthesis

4.4.2.1 Effect of acetic acid to ethanol ratio (A/E)

In this study, acetic acid and ethanol were chosen as a solvent mixture; the ratio of these two solvents might influence the formation of $Bi_4Ti_3O_{12}$. Thus, the A/E was investigated using various ratios, namely 0.1, 0.5, 1.0 and 1.5, while fixing the other parameters. It was found that a higher acetic acid content resulted in a longer gelation time. The FT-IR spectra of dried gel powders at different A/E values are shown in Fig. 3. The peaks at 1619 and 1549 cm^{-1} exhibited antisymmetric and symmetric stretching of COO_2 in the titanium acetate complex respectively.[22,23] At A/E >0.1, the antisymmetric peak was distorted while the intensity of the symmetric peak was increased. The frequency difference $\Delta\nu$ between antisymmetric and symmetric stretching of all samples was almost constant, 70 cm^{-1}, indicating that the acetate group functions as a bidentate ligand (chelating and bridging).[24] The peaks at 1384 (stretching of NO_3^- ion), 1380 (C–H stretching of organic components), 1000–1100 (C–O stretching) and 651 and 527 cm^{-1} (M–O stretching) were observed.[25,26]

In general, titanium butoxide is very reactive towards water, resulting in an uncontrollable sol–gel process. According to Xie and Pan,[27] titanium butoxide could easily react with acetic acid to form titanium complex containing acetate group (equation (1)), and the acetate group would then retard the hydrolysis reaction, causing easier control of the sol–gel process.

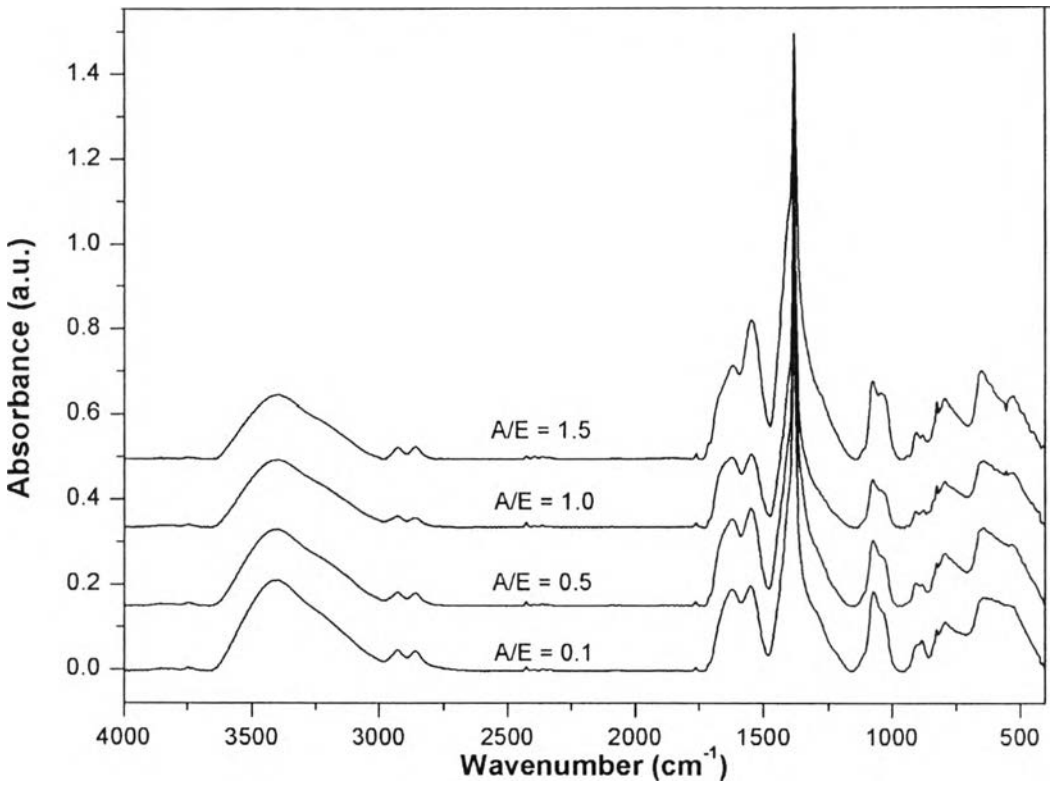

Figure 4.3 FT-IR spectra of the dried precursors using different acetic acid-to-ethanol ratios.

After acetic acid protonates butoxy group of the titanium complex, the hydrolysis reaction occurs

$$Ti(OC_4H_9)_4 + xCH_3COOH \rightarrow Ti(OC_4H_9)_{4-x}(CH_3COO)_x + xC_4H_9OH \quad (1)$$

Generally, bismuth nitrate salt easily reacts with water to yield white precipitate $BiONO_3$ powder[28]; thus, it is necessary to add a complexing agent, such as ethanolamine, to stabilise and control the hydrolysis of bismuth nitrate. Xie and Pan synthesised perovskite $BaBi_4Ti_4O_{15}$ and found that the pure perovskite powder could not be obtained without the addition of ethanolamine.[27] In our work, we illustrate the superiority of our home-made bismuth glycolate precursor over commercial $Bi(NO_3)_3.5H_2O$. One advantage of our precursor is its moisture stability, enabling control of its hydrolysis rate.

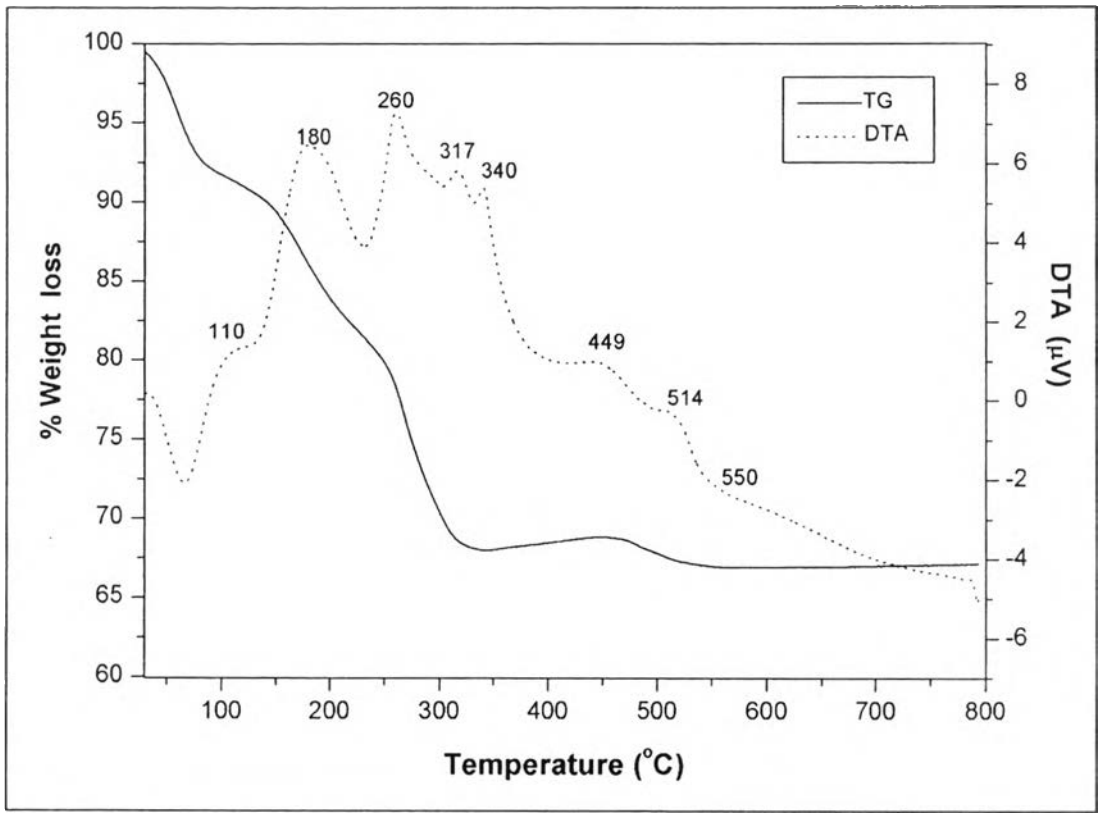

Figure 4.4 TG-DTA of sample using acetic acid-to-ethanol ratio of 0.1.

The thermal behavior of the dried gel powder synthesized with 0.1 A/E is shown in Figure 4.4. The first and the second weight losses at 80–100 and 100– 200 °C (~ 7.5% each) corresponded to the decomposition of adsorbed water and organic solvents, respectively.[29] The weight loss of ~ 17.5% at 200–341 °C is related to the decomposition of organic molecules in the gel network, correlating with the DTA curve at 260, 317, and 340° C.[30] The trace amount of weight loss around 449–550 °C in TG associated with the exothermic peak at 449 and 514 °C in DTA were assigned to the evaporation of the CO_2 from the decomposition of carbonate mixture, as also found in other sol–gel preparation processes.[29,31,32] Moreover, the small exothermic peak at 550 °C in DTA indicated complete conversion of amorphous to crystalline of the $Bi_4Ti_3O_{12}$ phase.[29] The XRD patterns of the as synthesised $Bi_4Ti_3O_{12}$ and calcined products are illustrated in Figure 4.5.

The perovskite single phase was obtained in all A/E ratios, illustrating an orthorhombic phase of $Bi_4Ti_3O_{12}$ according to JCPDS 35-795.

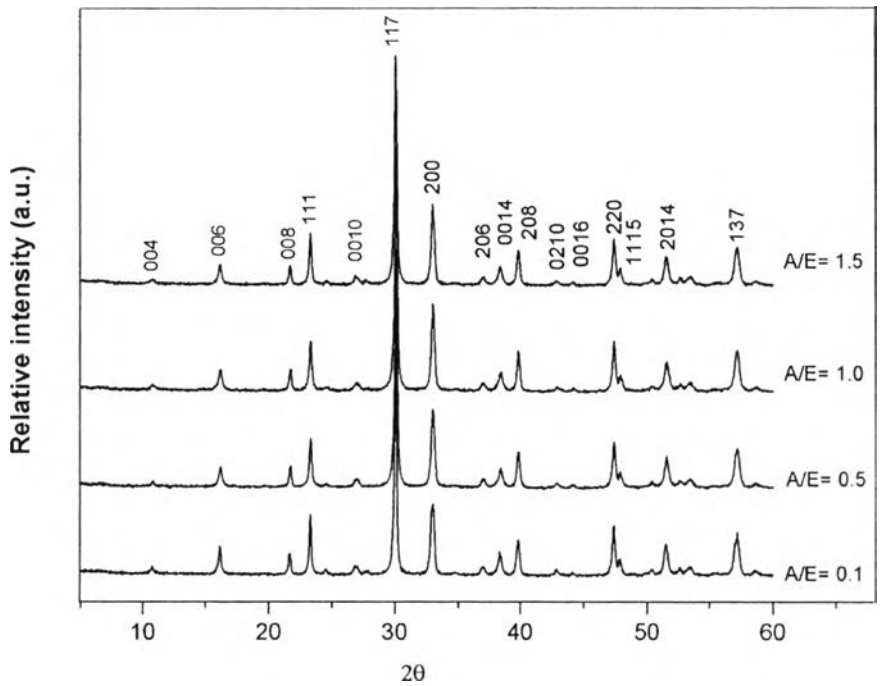

Figure 4.5 X-ray diffraction patterns of $Bi_4Ti_3O_{12}$ calcined at 600 °C for 1 h using different A/E ratios

4.4.2.2 Effect of calcination temperature

The dried gel powder was calcined at a temperature range of 300–700 °C for 1 h. The transformation phase of the product obtained was investigated by XRD, as shown in Figure 4.6. As synthesised $Bi_4Ti_3O_{12}$ clearly showed an amorphous phase, which slowly transformed into a crystalline phase at 300 °C calcination temperature due to the decomposition of organic and inorganic compounds, the amorphous phase of the as synthesized $Bi_4Ti_3O_{12}$ started to crystallise with increasing temperature. At 400°C, sillenite ($Bi_{12}TiO_{20}$) intermediate phase started to form, and then disappeared with an increase in temperature to 500°C, and perovskite ($Bi_4Ti_3O_{12}$) began to appear. The single phase of perovskite was obtained when the calcination temperature reached 600°C and remained stable up to

700°C. This observation is consistent with the work done by Fang et al.,[33] who synthesised $Bi_{3.25}La_{0.75}Ti_3O_{12}$ by complex polymerization method, in which the sillenite intermediate phase appeared as an impurity in the perovskite phase. Moreover, Navarro-Rojero et al.[34] studied intermediate phase formation during the synthesis of perovskite $Bi_4Ti_3O_{12}$ and proposed the formation of the intermediate, as follows

$$6Bi_2O_3 + 9TiO_2 \rightarrow Bi_{12}TiO_{20} \quad (2)$$

$$Bi_{12}TiO_{20} + 8TiO_2 \rightarrow 3Bi_4Ti_3O_{12} \quad (3)$$

Thus, in our work, when the calcination temperature reached 600°C, the amorphous titanium dioxide was diffused to sillenite intermediate grains to form perovskite $Bi_4Ti_3O_{12}$, consistent with the DTA data resulting in the transformation of the amorphous phase to complete crystalline phase at temperature ≥ 550 °C.

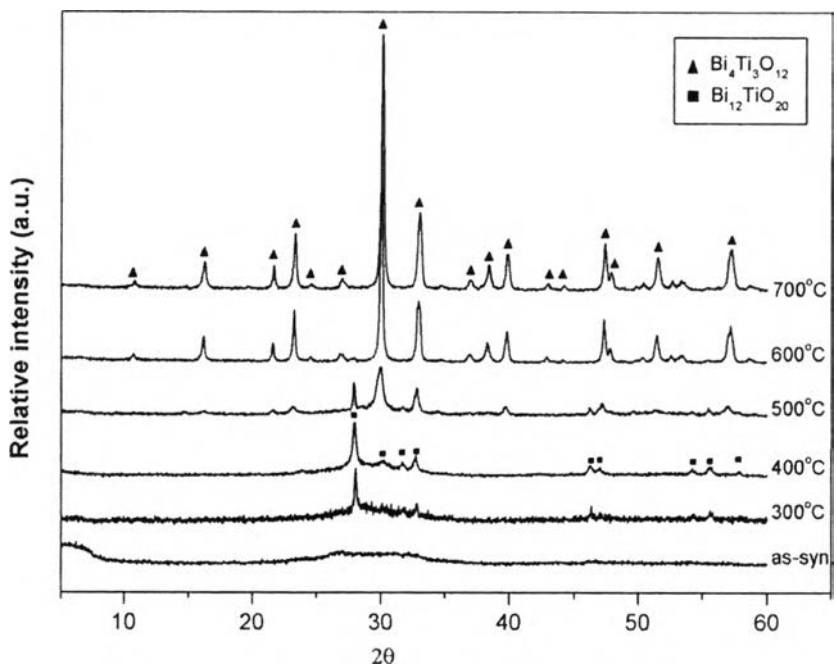

Figure 4.6 X-ray diffraction patterns of as synthesised and $Bi_4Ti_3O_{12}$ calcined at different temperatures.

4.4.2.3 Effect of mechanical stirring time

In the sol–gel process, mechanical stirring may also influence the colloidal formation, since the mechanical force from stirring could cause particle aggregation to break down and suspend in solution, affecting the gelation state and the quality of the final product. Thus, in this work, we conducted the experiment using various stirring times with 0.1 A/E and fixed other parameters. Figure 4.7 demonstrates the morphology of samples stirred for 1, 3 and 6 h. A nanoplate shaped $Bi_4Ti_3O_{12}$ was obtained in 1 h stirring time. After prolonging the stirring time to 3 and 6 h, the morphology became slightly distorted to smaller sized cubic particles. For more detailed investigation, the particles within the selected area of Figure 4.7c were enlarged from 60,000 to 150,000 magnification (Figure 4.7d), and it was found that an individual particle actually consisted of a number of thin plate particles. This agglomeration of $Bi_4Ti_3O_{12}$ thin plates was also observed by Hou et al.,[30] who stated that this agglomeration process of thin plate particles occurred through van der Waals force in order to reduce its surface energy.

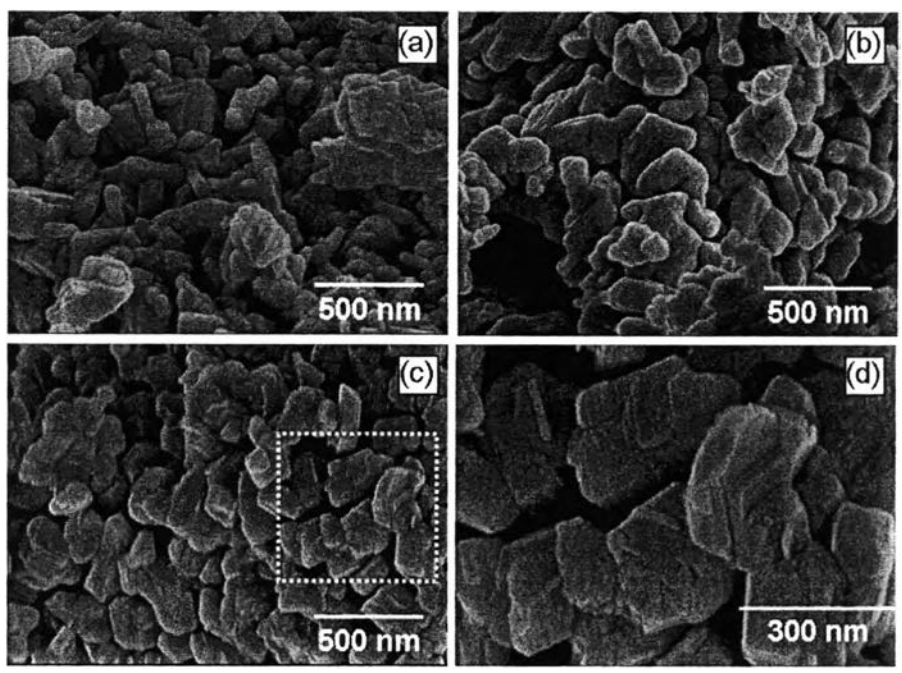

Figure 4.7 Images (SEM) of bismuth titanate obtained from using different stirring times of; (a) 1, (b) 3, and (c-d) 6 h with magnification of 60,000 and 150,000, respectively.

The calcined products of bismuth titanate were identified by XRD, as seen in Figure 4.8, showing the XRD patterns of bismuth titanate stirred for 1, 3, and 6 h. Only a single phase of the orthorhombic structure was achieved. Thus, a mechanical stirring time of 1 h is sufficient for dispersing the colloidal particles in the solution before changing to the gelation state.

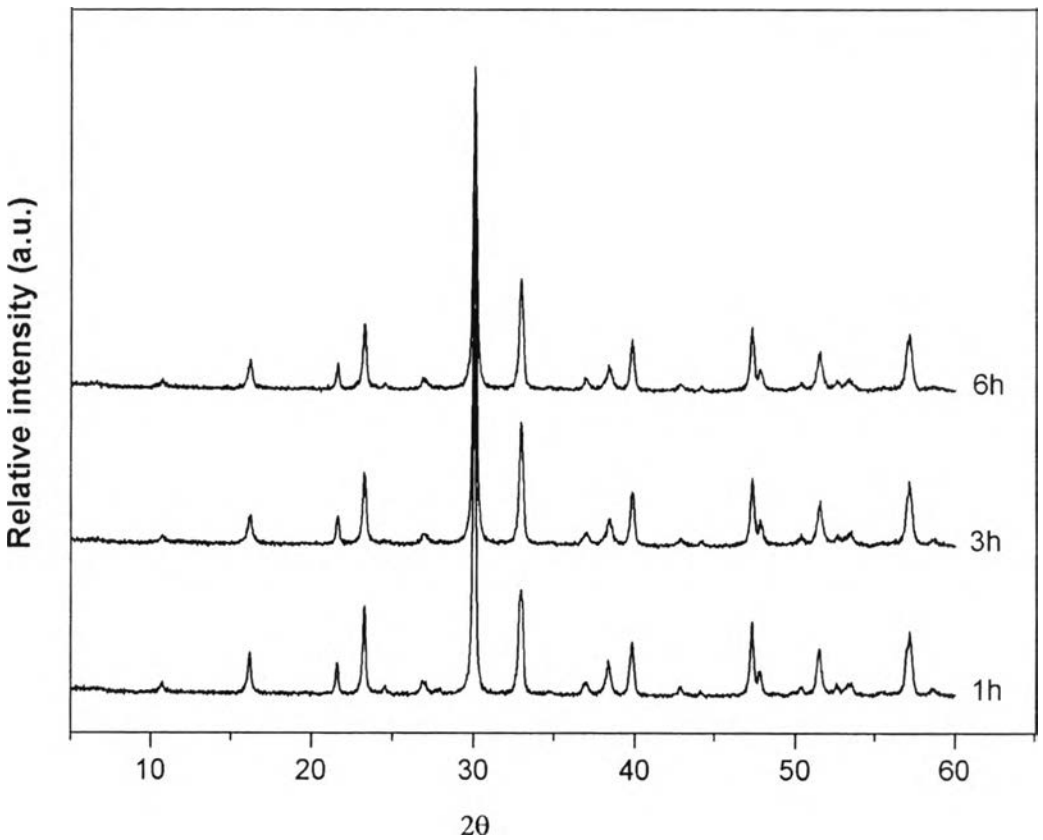

Figure 4.8 X-ray diffraction patterns of $Bi_4Ti_3O_{12}$ synthesized at different mechanical stirring times.

4.4.2.3 Effect of calcination time

The dried gel of $Bi_4Ti_3O_{12}$ was calcined at 600 °C for 1, 2 and 3 h. The results are shown in Figure 4.9. Obviously, higher calcination time led to higher crystallinity of the $Bi_4Ti_3O_{12}$ product without destroying the phase structure.

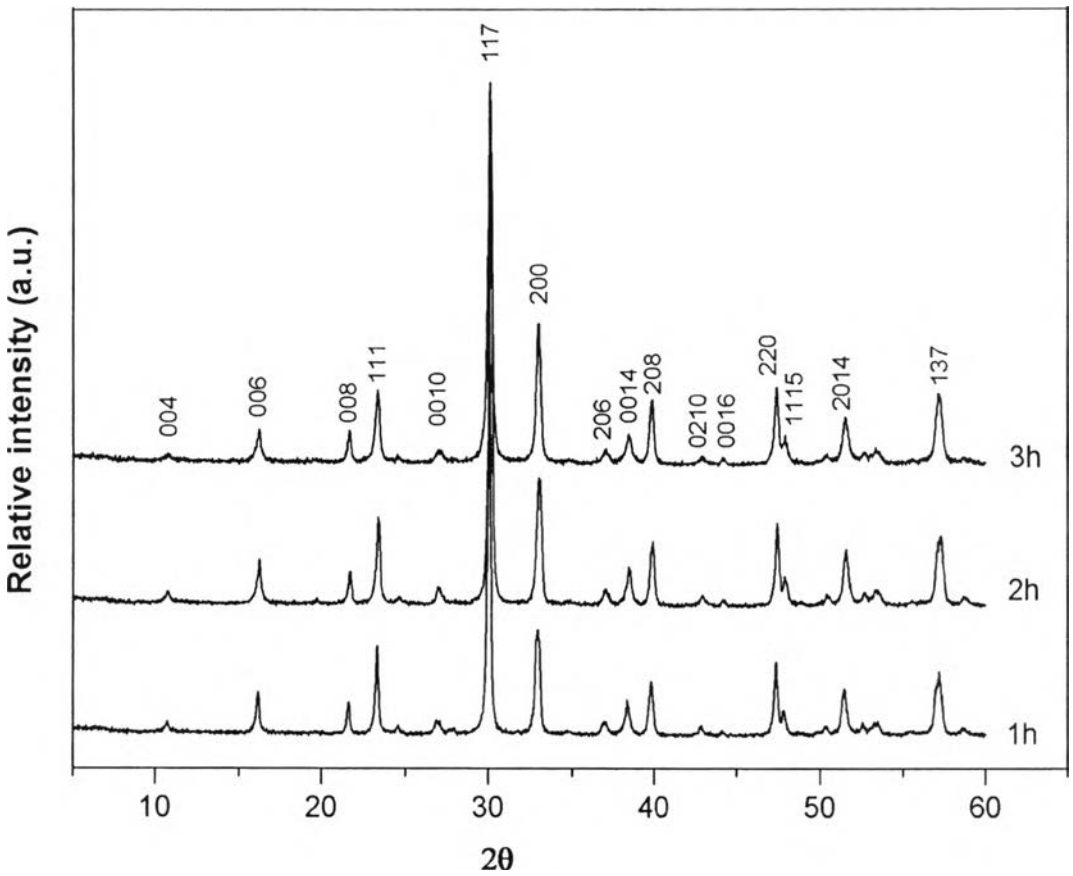

Figure 4.9 XRD patterns of $Bi_4Ti_3O_{12}$ calcined at 600 °C for a) 1, b) 2, and c) 3 h.

4.5 Conclusions

Bismuth titanate was successfully synthesised via sol–gel process using acetic acid–ethanol solvent mixture and bismuth glycolate precursor obtained by heating commercially available bismuth nitrate in EG for 1 h. The higher acetic acid content resulted in a longer gelation time with no effect on the perovskite phase formation. The single phase of perovskite with a plate-like shape was obtained at 600 °C.

4.6 Acknowledgments

This work was supported by the National Center of Excellence for Petroleum, Petrochemicals, and Advanced Materials, Chulalongkorn University. In addition, the authors would like to thank Mr John M. Jackson for English proofreading.

4.7 References

[1] B. Aurivillius, Mixed Bismuth Oxides with Lauer Lattices: I, Ark Kemi, 1949, 1, 463-471.

[2] 2. Q.Y. Tang, Y.M. Kan, Y.G. Li, G.J. Zhang and P.L. Wang, Ferroelectric and dielectric properties of Nd/V co-doped $Bi_4Ti_3O_{12}$ ceramics, Solid State Communications, 2007, 142, 1-5.

[3] C.M. Wang, J.F. Wang, Z.G. Gai, M.L. Zhao, L. Zhao, J.X Xu, N. Yin, C.J. Zhang, S.Q. Sun, G.Z. Zang, R.Q. Chu and Z.J. Xu, Ferroelectric, dielectric and piezoelectric properties of potassium lanthanum bismuth titanate $K_{0.5}La_{0.5}Bi_4Ti_4O_{15}$ ceramics, Materials Chemistry and Physics, 2008, 110, 402-405.

[4] G.B. Kumar and S. Buddhudu, Optical, thermal and dielectric properties of $Bi_4(TiO_4)_3$ ceramic powders, Ceramics International, 2010, 36, 1857-1861.

[5] M.F. Carrasco, S.K. Mendiratta and L. Marques, Formation of an intermediate phase in the ball milling synthesis of the sillenite phase of BSO and BTO, Applied Physics A: Materials Science & Processing, 2005, 80, 361-367.

[6] H. Gu, Z. Hu, Y. Hu, Y. Yuan, J. You and W. Zou, The structure and photoluminescence of $Bi_4Ti_3O_{12}$ nanoplates synthesized by hydrothermal method, Colloid and Surfaces Sciences A: Physicochemical and Engineering Aspect, 2008, 315, 294-298.

[7] Z.C. Ling, H.R. Xia, W.L. Liu, H. Han, X.Q. Wang, S.Q. Sun, D.G. Ran and L.L. Yu, Lattice vibration of bismuth titanate nanocrystals prepared by metalorganic decomposition, Materials Science and Engineering B, 2006, 128, 156-160.

[8] A.M. Umabala, M. Suresh and A.V. Prasadarao, Bismuth titanate from coprecipitated stoichiometric hydroxide precursors, Materials Letters, 2000, 44, 175-180.

[9] S. Madeswaran, N.V. Giridharan and R. Jayavel, Sol–gel synthesis and property studies of layered perovskite bismuth titanate thin films, Materials Chemistry and Physics, 2003, 80, 23-28.

[10] L. Pei, M. Li, J. Lui, B. Yu, J. Wang and X. Zhao, Improvements of the ferroelectric properties of high-valence Tb-doped $Bi_4Ti_3O_{12}$ thin film grown by sol–gel method, Materials Letters, 2010, 64, 364-366.

[11] H. Shen, Q. Guo, Z. Zhao and G. Cao, Sol–gel derived PZT films doped with vanadium pentoxide, Materials Research Bulletin, 2009, 44, 2152-2154.

[12] D.H. Kang, B.S. Lee, H.K. An, Y.H. Kim, D.S. Paik, H.I. Hwang and N.K. Cho, Characteristics of yttrium substituted sodium bismuth titanate thin films, Materials Letters, 2010, 64, 2331-2333.

[13] A. Haaland, H.P. Verne, H.V. Volden, R. Papiernik and L.G. Hubert-Pfalzgraf, Molecular structure of a monomeric bismuth trisalkoxide by gas electron diffraction, Acta Chemica Scandinavica, 1993, 47, 1043-1045.

[14] S. Shimada, M.L.N. Rao and M. Tanaka, Synthesis and structure of monoorganobismuth compounds bearing pyridinedimethoxide ligands, Organometallics., 2000, 19, 931-936.

[15] M.C. Massiani, R. Papiernik, L.G. Hubert-Pfalzgraf and J.C. Daran, Molecular precursors of bismuth oxides; β-Diketonates and alkoxides. Molecular structure of $[Bi_2(\mu_2,\eta^1\text{-}OC_2H_4OMe)_4\ (\eta^1\text{-}OC_2H_4OMe)_2]_\infty$ and of $Bi(OSiPh_3)_3(THF)_3$, Polyhedron, 1991, 10, 437-445.

[16] C. Goia, E. Matijević and D.V. Goia, Preparation of colloidal bismuth particles in polyols, Journal of Materials Research, 2005, 20, 1507-1514.

[17] J. Li, H. Fan, J. Chen and L. Liu, Synthesis and characterization of poly(vinyl pyrrolidone)-capped bismuth nanospheres, Colloid and Surfaces Sciences A: Physicochemical and Engineering Aspect, 2009, 340, 66-69.

[18] R.P. Oertel and R.A. Plane, Raman and infrared study of nitrate complexes of bismuth(III), Inorganic Chemistry, 1968, 7, 1192-1196.

[19] T. Zevaco and M. Postel, Bismuth (III) Complexes from Glycol and α-Hydroxycarboxylic acids, Synthesis and Reactivity in Inorganic and Metal-Organic Chemistry, 1992, 22, 289-297.

[20] N. Chakroune, G. Viau, S. Ammar, N. Jouini, P. Gredin, M.J. Vaulay and F. Fievet, Synthesis, Characterization and magnetic properties of disk-shaped particles of a cobalt alkoxide: $Co^{II}(C_2H_4O_2)$, New journal of chemistry, 2005, 29, 355-361.

[21] D. Larcher, B. Gerand and J.M. Tarascon, Synthesis and electrochemical performances of $Li_{1+y}Mn_{2-y}O_4$ powders of well-defined morphology, Journal of Solid State Electrochemistry, 1998, 2, 137-145.

[22] S. Doeuff, M.Henry, C. Sanchez and J. Livage, Hydrolysis of titanium alkoxides: Modification of the molecular precursor by acetic acid, Journal of Non-Crystalline Solids, 1987, 89, 206-216.

[23] R. Sui, A.S. Rizkalla and P.A. Charpentier, FTIR study on the formation of TiO_2 nanostructures in supercritical CO_2, The Journal of Physical Chemistry B, 2006, 110, 16212-16218.

[24] F.X. Perrin, V. Nguyen and J.L. Vernet, FT-IR spectroscopy of acid-modified titanium alkoxides: investigations on the nature of carboxylate coordination and degree of complexation, Journal of Sol-Gel Science and Technology, 2003, 28, 205-215.

[25] T. Thongtem and S. Thongtem, Characterization of $Bi_4Ti_3O_{12}$ powder prepared by the citrate and oxalate coprecipitation processes, Ceramics International, 2004, 30, 1463-1470.

[26] K. Nakamoto, in, Infrared and raman spectra of inorganic and coordination compounds: Part B: applications in coordination, organometallic, and bioinorganic, 5th edn, 75; 1997, New York, Wiley.

[27] D. Xie and W. Pan, Study on $BaBi_4Ti_4O_{15}$ nanoscaled powders prepared by sol–gel method, Materials Letters, 2003, 57, 2970-2974.

[28] H. Gu, P. Chen, Y. Zhou, M. Zhao, A. Kuang and X. Li, Reactions in preparing $Bi_4Ti_3O_{12}$ ultrafine powders by sol-gel process, Ferroelectrics, 1998, 211, 271-280.

[29] H. Ke, W. Wang, L. Chen, J. Xu, D. Jia, Z. Lu and Y. Zhou, Crystallization process of lanthanum-substituted bismuth titanate synthesized by a facile sol-gel method, Journal of Sol-Gel Science and Technology, 2010, 53, 135-140.

[30] J. Hou, R.V. Kumar, Y. Qu and D. Krsmanovic, Controlled synthesis of photoluminescent $Bi_4Ti_3O_{12}$ nanoparticles from metal-organic polymeric precursor, Journal of Nanoparticle Research, 2010, 12, 563-571.

[31] H. Ke, Y. Zhou, D.C. Jia, W. Wang, X.Q. Xu and F. Ye, Crystallization and Nanograin Growth in $SrBi_2Ta_2O_9$ Synthesized by a Novel Sol–Gel Process, Journal of Sol-Gel Science and Technology, 2005, 34, 131-136.

[32] K. Huang, M. Feng and J.B. Goodenough, Sol-gel synthesis of a new oxide-ion conductor Sr- and Mg-doped $LaGaO_3$ perovskite, Journal of the American Ceramic Society, 1996, 79, 1100-1104.

[33] P. Fang, H. Fan, S. Qiu, L. Liu and J. Chen, $Bi_{3.25}La_{0.75}Ti_3O_{12}$ powders by the complex polymerization method: synthesis, characterization and morphology, Journal of Sol-Gel Science and Technology, 2009, 50, 290-295.

[34] M.G. Navarro-Rojero, J.J. Romero, F. Rubio-Marcos and J.F. Fernandez, Intermediate phases formation during the synthesis of $Bi_4Ti_3O_{12}$ by solid state reaction, Ceramics International, 2010, 36, 1319-1325.